# Comprehensive Analysis of Immune Cell Enrichment in the Tumor Microenvironment of Head and Neck Squamous Cell Carcinoma

**Ikko Mito**
Gunma University Graduate School of Medicine School of Medicine: Gunma Daigaku Daigakuin Igakukei Kenkyuka Igakubu

**Hideyuki Takahashi** ( htakahas@gunma-u.ac.jp )
Gunma University Graduate School of Medicine School of Medicine: Gunma Daigaku Daigakuin Igakukei Kenkyuka Igakubu https://orcid.org/0000-0002-2465-3992

**Reika Kawabata-Iwakawa**
Gunma University Initiative for Advanced Research

**Shota Ida**
Gunma University Graduate School of Medicine School of Medicine: Gunma Daigaku Daigakuin Igakukei Kenkyuka Igakubu

**Hiroe Tada**
Gunma University Graduate School of Medicine School of Medicine: Gunma Daigaku Daigakuin Igakukei Kenkyuka Igakubu

**Kazuaki Chikamatsu**
Gunma University Graduate School of Medicine School of Medicine: Gunma Daigaku Daigakuin Igakukei Kenkyuka Igakubu

**Primary research**

**Keywords:** head and neck squamous cell carcinoma, immunosuppression, tumor microenvironment, immune checkpoint, TCGA

**Posted Date:** May 17th, 2021

**DOI:** https://doi.org/10.21203/rs.3.rs-517086/v1



**Version of Record:** A version of this preprint was published at Scientific Reports on August 9th, 2021. See the published version at https://doi.org/10.1038/s41598-021-95718-9.

# Abstract

**Background:** Head and neck squamous carcinoma (HNSCC) is highly infiltrated by immune cells, including tumor-infiltrating lymphocytes and myeloid lineage cells. In the tumor microenvironment, tumor cells orchestrate a highly immunosuppressive microenvironment by secreting immunosuppressive mediators, expressing immune checkpoint ligands, and downregulating human leukocyte antigen expression. In the present study, we aimed to comprehensively profile the immune microenvironment of HNSCC using RNA-sequencing (RNA-seq) data obtained from The Cancer Genome Atlas (TCGA) database.

**Methods:** We calculated enrichment scores of 33 immune cell types based on RNA-seq data of HNSCC tissues and adjacent non-cancer tissues. Based on these scores, we performed non-supervised clustering and identified three immune signatures, i.e., cold, lymphocyte, and myeloid/dendritic cell (DC), using clustering results. We then compared the clinical and biological features of the three signatures.

**Results:** Among HNSCC and non-cancer tissues, human papillomavirus (HPV)-positive HNSCCs exhibited the highest scores in various immune cell types, including CD4+ T cells, CD8+ T cells, B cells, plasma cells, basophils, and their subpopulations. Among the three immune signatures, the proportions of HPV-positive tumors, oropharyngeal cancers, early T tumors, and N factor positive cases were significantly higher in the lymphocyte signature than in other signatures. Among the three signatures, the lymphocyte signature showed the longest overall survival (OS), especially in HPV-positive patients, whereas the myeloid/DC signature demonstrated the shortest OS in these patients. Gene set enrichment analysis revealed the upregulation of several pathways related to inflammatory and proinflammatory responses in the lymphocyte signature. The expression of *PRF1*, *IFNG*, *GZMB*, *PDCD1*, *LAG3*, *CTLA4*, *HAVCR2*, and *TIGIT* was the highest in the lymphocyte signature. Meanwhile, the expression of PD-1 ligand genes *CD274* and *PDCD1LG2* was highest in the myeloid/DC signature.

**Conclusions:** Herein, our findings revealed the transcriptomic landscape of the immune microenvironment that closely reflects the clinical and biological significance of HNSCC, indicating that molecular profiling of the immune microenvironment can be employed to develop novel biomarkers and precision immunotherapies for HNSCC.


# Background

Head and neck squamous cell carcinoma (HNSCC) is the sixth most common malignant tumor worldwide [1, 2]. In addition to tobacco-derived carcinogens and excessive alcohol consumption, infection with oncogenic strains of human papillomavirus (HPV) has been recognized as a major risk factor for developing HNSCCs, mainly oropharyngeal cancers [3, 4]. Despite ongoing improvements in therapeutic strategies, including surgery, chemotherapy, and radiotherapy, the 5-year survival rate remains 66%. Recently, cancer immunotherapy has been developed as an additional approach for various cancer types, including HNSCC [5-7]. The programmed cell death 1/programmed cell death ligand 1 (PD-1/PD-L1) axis

is a crucial target for immune checkpoint therapies [8]. In clinical settings, anti-PD-1 antibodies have been widely employed for treating recurrent or metastatic HNSCC; however, survival benefits have been observed in only 20%–30% of patients. Accordingly, novel biomarkers have been widely investigated to improve the efficacy of immunotherapies.

In the tumor microenvironment (TME), various stromal cells such as immune cells, fibroblasts, and endothelial cells exist and interact with tumor cells [9, 10]. HSNCC is highly infiltrated by immune cells, including tumor-infiltrating lymphocytes (TILs) and myeloid lineage cells [11, 12]. In the TME of HNSCC, tumor cells reportedly orchestrate a highly immunosuppressive state by secreting immunosuppressive mediators, expressing immune checkpoint ligands, and downregulating human leukocyte antigen expression [13, 14]. These tumor cell behaviors result in the dysfunction and exhaustion of cytotoxic T lymphocytes (CTLs), as well as increased infiltration and activation of immunosuppressive cell types, such as regulatory T cells (Tregs), tumor-associated macrophages, and myeloid-derived suppressor cells (MDSCs) [15]. As immune checkpoint agents target the interaction between tumor cells and immune cells, a comprehensive analysis of the complex state of the immune microenvironment would be beneficial for developing new biomarkers and precision immunotherapies.

In the present study, we aimed to comprehensively profile the immune microenvironment of HNSCC using RNA-sequencing (RNA-seq) data obtained from The Cancer Genome Atlas (TCGA) database. We calculated the cell enrichment scores of 33 immune cell types based on RNA-seq data of both HNSCC tissues and adjacent non-cancer tissues. Based on these scores, we performed non-supervised clustering and identified three immune signatures—cold, lymphocyte, and myeloid/dendritic cell (DC)—based on clustering results. Finally, the clinical and biological features of the three signatures were compared.

# Materials And Methods

### Acquisition of The Cancer Genome Atlas (TCGA) data

RNA-seq data (Illumina Hiseq RNAseq V2, raw counts, and normalized counts) and clinical data were obtained from TCGA Research Network (TCGA Provisional version updated in 2016, http://cancergenome.nih.gov/). In total, 564 cases, consisting of 44 normal samples, 97 HPV-positive HNSCC, and 423 HPV-negative HNSCC, were included.

### Cell type enrichment analysis

We performed cell type enrichment analysis to evaluate the enrichment of 33 immune cell types in 520 HNSCC tissues and 44 normal tissues using the xCell tool [16]. Enrichment scores were calculated using the xCell R package, version 1.1.0. The calculated scores were visualized using the pheatmap R package, version 1.10.12. Then, normal and HNSCC tissue scores were compared.

### Non-supervised hierarchical clustering of HNSCC samples

HNSCC cases underwent non-supervised hierarchical clustering based on cell enrichment scores of 33 immune cell types. Patients were then divided into three immune signatures, cold, lymphocyte, and myeloid/DC, based on the clustering results. The three signatures were compared in terms of clinical parameters, including HPV status, primary lesion, T factor, N factor, M factor, tumor-node-metastasis (TNM) stage, disease-free survival (DFS), and overall survival (OS). The three signatures were also compared to the normalized gene expression of various immune-related genes.

### Differentially expressed gene analysis

Next, we compared differentially expressed genes (DEGs) between the lymphocyte signature group and other signature groups, using the ExperimentHub R package version 1.16.0 and DESeq2 R package version 1.30.0. DEGs were filtered using the threshold $|\log_2 FC| \geq 1$ and an adjusted *P*-value of<0.05. Volcano plots were constructed to visualize DEGs using the calibration R package version 1.7.7.

### Gene set enrichment analysis

Gene set enrichment analysis (GSEA; GSEA v4, Broad Institute) was performed to identify pathways upregulated in the lymphocyte group when compared with other groups. For each gene set, the normalized enrichment score, *P*-value, and false discovery rate (FDR) q-values were calculated based on the Hallmark pathway database.

### Statistical analysis

Data were analyzed using R (version 4.0.3; The R Foundation for Statistical Computing, Vienna, Austria) in combination with R studio version 1.3.1093 (R studio, Boston, MA, USA) and GraphPad Prism version 8 (GraphPad Software, San Diego, CA, USA). Student's t-test and one-way ANOVA with Tukey's post-hoc test for multiple pairwise testing were employed to compare continuous variables between groups. The Chi-square test for independence and Fisher's exact test were used for comparing categorical variables. Two-sided *P*-values of <0.05 were considered statistically significant. Survival curves were calculated using the Kaplan-Meier method and compared using the log-rank test.

## Results

### HPV-positive HNSCCs exhibited upregulated enrichment of various immune cells

We calculated the enrichment scores of 33 immune cell types among 520 HNSCCs and 44 normal samples (Figure 1, Suppl. Figure 1). HPV-positive HNSCCs exhibited the highest scores for various immune cell types, including CD4+ T cells, CD8+ T cells, B cells, plasma cells, basophils, as well as their subpopulations. Normal samples exhibited the lowest scores for several cell types.

### The lymphocyte signature correlated with clinical parameters and better prognosis

Based on hierarchical clustering results, we segregated 520 HNSCCs into three immune signatures (Figure 2a). The lymphocyte signature was characterized by the enrichment of CD4+ T cells, CD8+ T cells, B cells, and plasma cells (Figure 2b, Suppl. Figure 2). The myeloid/DC signature exhibited enrichment of neutrophils, macrophages, monocytes, DCs, Tregs, and eosinophils (Figure 2b, Suppl. Figure 2). Table 1 presents correlations between immune signatures and clinical parameters. The proportion of HPV-positive patients (59%) was significantly higher in the lymphocyte signature than in other signatures. Regarding primary lesions, the proportion of the oropharynx (50%) was higher in the lymphocyte signature than in other signatures. The proportion of patients with early T factor (63%) was higher in the lymphocyte signature than in other signatures. Furthermore, the proportion of N factor-positive patients (61%) was higher in the lymphocyte signature than other signatures. No difference was observed between immune signatures and the M factor/TNM stage. Survival analyses revealed that the lymphocyte signature showed the longest OS among the three signatures, especially in HPV-positive patients (Figure 2c). The myeloid/DC signature showed the shortest OS among the three signatures in HPV-positive patients. No difference in DFS was observed between immune signatures.

### The lymphocyte signature correlated with inflammatory pathways

Based on these findings, we then focused on the transcriptomic significance of the lymphocyte signature. In the lymphocyte signature, 3330 DEGs, including 1831 upregulated and 1499 downregulated genes, were identified (Figure 3a, Suppl. Table 1). Additionally, we performed GSEA to identify pathways upregulated in the lymphocyte signature (Figure 3b). In the lymphocyte signature, 8 hallmark pathways were upregulated, whereas 12 were downregulated (FDR□0.05). Several pathways associated with inflammatory and proinflammatory responses, such as allograft rejection, interferon (IFN) gamma response, interleukin (IL) 6-Janus kinase (JAK)-signal transducer and activator of transcription (STAT) 3 signaling, interferon-alpha response, IL2 STAT5 signaling, and complement, were upregulated in the lymphocyte signature. Meanwhile, several pathways representing malignant features of HNSCCs, including hypoxia, angiogenesis, transforming growth factor (TGF)-β signaling, and epithelial-mesenchymal transition, were downregulated in the lymphocyte signature.

### The lymphocyte signature correlated with activated cytotoxic T cell response

We investigated the expression of immune-related genes to compare cytotoxic T cell responses across the three immune signatures (Figure 3c). The lymphocyte signature demonstrated the highest expression of genes related to cytotoxic T cell responses, including *PRF1*, *IFNG*, and *GZMB*. Additionally, the expression of immune checkpoint genes, including *PDCD1*, *LAG3*, *CTLA4*, *HAVCR2*, and *TIGIT*, was the highest in the lymphocyte signature. Meanwhile, the expression of PD-1 ligand genes *CD274* and *PDCD1LG2* was the highest in the myeloid/DC signature, which also revealed the highest expression of immunosuppressive genes, *TGFB1* and *IL10*.

## Discussion

Recent advances in bioinformatics and the accumulation of public genomic databases have enabled the comprehensive genomic characterization of cancer in a large cohort [17]. In the present study, we elucidated the transcriptomic landscape of the immune microenvironment that closely reflects the clinical and biological significance of HNSCC. Our results suggest that molecular profiling of the immune microenvironment can potentially help develop new biomarkers and precision immunotherapies.

The comparison of immune cell enrichment scores revealed high infiltration of various immune cells into HNSCC tissues, especially in HPV-positive HNSCCs. The scores of various TILs were higher in HNSCCs than in normal tissues. Among TILs, CD8+ T cells are the main subset of CTLs and play vital roles in tumor eradication. CD8+ T cells, as well as their subset CD8+ central memory T cells (Tcm) and CD8+ effector memory T cells (Tem), presented significantly higher scores in HPV-positive HNSCCs than in other groups, indicating a highly activated CTL function in the TME of HPV-positive HNSCCs [18, 19]. Consistent with our results, accumulating evidence suggests that HPV-positive HNSCCs correlate with T cell-enriched TME, increased T cell receptor pathway signaling, activated cytotoxic capacity, and viral antigen-specific CD8+ T cell infiltration into the TME [20-22]. Additionally, we observed a significant increase in B cell subsets and plasma cells in HPV-positive tumors but not in HPV-negative tumors. Although the significance of B cell infiltration in the TME is not well understood, recent studies have reported the anti-tumor activity of B cells and plasma cells through antigen presentation and antibody production [23]. A recent study reported the presence of HPV-specific antibody-secreting cells in the TME of HPV-positive tumors [24]. Moreover, Kim et al. have reported that B cells correlate with longer OS and are activated by radiation and PD-1 blockade therapy [25]. These findings suggest the potential of B-cell-targeted immunotherapy. Further investigations regarding the specific roles of B cells and plasma cells in the TME are warranted.

Herein, non-supervised clustering of HNSCC cases based on the cell enrichment scores of 33 immune cell types revealed three immune signatures: cold, lymphocyte, and myeloid/DC. The lymphocyte signature correlated with the HPV-positive type, early T factor, positive N factor, and favorable prognosis. Notably, the presence of T cell subsets has been widely investigated in several malignancies [26-30]. In HNSCC, the presence of TILs in the TME is reportedly considered a favorable prognostic factor [31, 32]. Moreover, Tsujikawa et al. have previously assessed immune cell complexity profiles of 38 HNSCC cases using multiplex immunohistochemistry [33]. They acquired cell densities of 15 immune cell lineages using image cytometry, followed by normalization and unsupervised hierarchical clustering. Their analysis revealed three immune signatures: lymphoid-inflamed, myeloid-inflamed, and hypo-inflamed. The myeloid-inflamed signature exhibited significantly shorter OS. In addition, the lymphoid-inflamed signature consisted of more HPV-positive HNSCCs than the other signatures. Surprisingly, the results of the present study are consistent with those of their protein expression-based analysis. Although bulk RNA sequencing cannot evaluate the localization of each immune cell in the TME, our results suggest that bulk RNA sequencing-based molecular profiling of immune cell complexity is equivalent to protein expression-based profiling, such as multiplex IHC. In addition to Tsujikawa's work, our results revealed that the myeloid/DC signature dramatically correlates with shorter OS in HPV-positive HNSCCs but not in HPV-negative cases. HPV-positive HNSCCs are widely recognized to exhibit a better prognosis than HPV-

negative HNSCCs [34, 35]. However, in clinical settings, some HPV-positive HNSCCs present aggressive behavior, resulting in a poor prognosis. Therefore, biomarkers that indicate the aggressive phenotype of HPV-positive HNSCCs are needed. The screening for myeloid-enriched TME has the potential to predict survival and allow precision medicine in HPV-positive HNSCCs.

We further focused on the transcriptomic significance of immune signatures. GSEA revealed the upregulation of multiple pathways related to inflammatory and proinflammatory responses, as well as the downregulation of pathways closely related to cancer hallmarks in the lymphocyte signature, as shown in Figure 3b. The upregulation of IFN-α responses, IFN-γ, and IL2 STAT5 signaling represents activated CTL responses, consistent with the presence of abundant lymphocytes. Furthermore, the lymphocyte signature showed the highest expression of both cytotoxic response-related genes *PRF1*, *IFNG*, and *GZMB*, and immune checkpoint genes *PDCD1*, *LAG3*, *CTLA4*, *HAVCR2*, and *TIGIT*. As these immune checkpoint molecules reportedly function as receptors for T cell inactivation and exhaustion signals, these molecules are abundantly expressed on effector memory T cells and tissue-resident memory T cells, which are activated phenotypes of T cells [36-39]. Accordingly, PD-1-expressing TILs are reportedly considered a favorable prognostic biomarker in HPV-positive HNSCCs [40]. Overall, the lymphocyte signature represented the enrichment of lymphocyte infiltration, activation of CTL functions, and favorable prognosis, especially in HPV-positive HNSCCs. As the cost of RNA sequencing has recently decreased, molecular profiling of the immune microenvironment using biopsy tissues may provide an alternative for the initial diagnosis of HNSCCs. However, in bulk RNA sequencing, the localization of immune cells cannot be determined. Dual profiling using both molecular and protein-based profiling would be helpful in comprehensively profiling the complexity of the immune milieu of the TME.

# Conclusions

The present study revealed the transcriptomic landscape of the immune microenvironment that closely reflects the clinical and biological significance of HNSCC. Our results suggest that molecular profiling of the immune microenvironment can be employed for developing new biomarkers and precision immunotherapies for HNSCC.

# Abbreviations

HNSCC: Head and neck squamous carcinoma

HPV: Human papillomavirus

PD-1: Programmed cell death 1

PD-L1: Programmed cell death ligand 1

TME: Tumor microenvironment

TIL: Tumor-infiltrating lymphocyte

CTL: Cytotoxic T lymphocyte

Treg: Regulatory T cell

MDSC: Myeloid-derived suppressor cell

RNA-seq: RNA-sequencing

TCGA: The Cancer Genome Atlas

DC: Dendritic cell

TNM: Tumor-node-metastasis

DFS: Disease-free survival

OS: Overall survival

DEG: Differentially expressed gene

GSEA: Gene set enrichment analysis

FDR: False discovery rate

IFN: Interferon

IL: Interleukin

JAK: Janus kinase

STAT: Signal transducer and activator of transcription

TGF: Transforming growth factor

Tcm: Central memory T cell

Tem: Effector memory T cell

# Declarations

**Ethics approval and consent to participate:** This is a retrospective trial from public datasets with minimal risk, and we petition for a waiver of ethics consent.

**Consent for publication:** This is a retrospective trial from public datasets with minimal risk, and we petition for a waiver of ethics consent.

**Availability of data and materials:** All data were obtained from TCGA Research Network (TCGA Provisional version updated in 2016, http://cancergenome.nih.gov/).

**Competing interests:** The authors declare no potential conflicts of interest.

**Funding:** This work was supported in part by a Grant-in-Aid for Scientific Research (B) 20H03834 (KC), Grant-in-Aid for Early-Career Scientists 19K18758 (IM), and Grant-in-Aid for Early-Career Scientists 20K18243 (HT) from the Ministry of Education, Culture, Sports, Science and Technology, Japan.

**Author contributions:** IM, investigation, software, formal analysis, funding acquisition, writing – initial draft preparation; HT, conceptualization, methodology, validation, resources, project administration, funding acquisition, writing – review and editing; RK, methodology, resources, writing – review and editing, visualization; SI, software, formal analysis; HT, software, formal analysis; KC, writing – review and editing, supervision, funding acquisition.

**Acknowledgments:** We would like to thank Dr. Yuki Saito and Dr. Koji Ebisumoto for teaching TCGA dataset manipulation.

# References

1. Ferlay J, Colombet M, Soerjomataram I, Mathers C, Parkin DM, Piñeros M, Znaor A, Bray F. Estimating the global cancer incidence and mortality in 2018: GLOBOCAN sources and methods. Int J Cancer. 2019;144(8):1941–53.
2. Bray F, Ferlay J, Soerjomataram I, Siegel RL, Torre LA, Jemal A. Global cancer statistics 2018: GLOBOCAN estimates of incidence and mortality worldwide for 36 cancers in 185 countries. CA Cancer J Clin. 2018;68(6):394–424.
3. Hashibe M, Brennan P, Benhamou S, Castellsague X, Chen C, Curado MP, Dal Maso L, Daudt AW, Fabianova E, Fernandez L, et al. Alcohol drinking in never users of tobacco, cigarette smoking in never drinkers, and the risk of head and neck cancer: Pooled analysis in the International Head and Neck Cancer Epidemiology Consortium. J Natl Cancer Inst. 2007;99(10):777–89.
4. Mehanna H, Beech T, Nicholson T, El-Hariry I, McConkey C, Paleri V, Roberts S. Prevalence of human papillomavirus in oropharyngeal and nonoropharyngeal head and neck cancer—Systematic review and meta-analysis of trends by time and region. Head Neck. 2013;35(5):747–55.
5. Couzin-Frankel J. Breakthrough of the year 2013. Cancer immunotherapy. Science. 2013;342(6165):1432–3.
6. Ferris RL, Blumenschein G, Fayette J, Guigay J, Colevas AD, Licitra L, Harrington K, Kasper S, Vokes EE, Even C, et al. Nivolumab for recurrent squamous-cell carcinoma of the head and neck. N Engl J Med. 2016;375(19):1856–67.
7. Burtness B, Harrington KJ, Greil R, Soulières D, Tahara M, de Castro G, Psyrri A, Basté N, Neupane P, Bratland Å, et al. Pembrolizumab alone or with chemotherapy versus cetuximab with chemotherapy

for recurrent or metastatic squamous cell carcinoma of the head and neck (KEYNOTE-048): A randomised, open-label, phase 3 study. Lancet. 2019;394(10212):1915–28.

8. Topalian SL, Hodi FS, Brahmer JR, Gettinger SN, Smith DC, McDermott DF, Powderly JD, Carvajal RD, Sosman JA, Atkins MB, et al. Safety, activity, and immune correlates of anti-PD-1 antibody in cancer. N Engl J Med. 2012;366(26):2443–54.
9. Labani-Motlagh A, Ashja-Mahdavi M, Loskog A. The tumor microenvironment: A milieu hindering and obstructing antitumor immune responses. Front Immunol. 2020;11:940.
10. Joyce JA. Therapeutic targeting of the tumor microenvironment. Cancer Cell. 2005;7(6):513–20.
11. Partlová S, Bouček J, Kloudová K, Lukešová E, Zábrodský M, Grega M, Fučíková J, Truxová I, Tachezy R, Špíšek R, et al. Distinct patterns of intratumoral immune cell infiltrates in patients with HPV-associated compared to non-virally induced head and neck squamous cell carcinoma. Oncoimmunology. 2015;4(1):e965570.
12. Mandal R, Şenbabaoğlu Y, Desrichard A, Havel JJ, Dalin MG, Riaz N, Lee KW, Ganly I, Hakimi AA, Chan TA, et al. The head and neck cancer immune landscape and its immunotherapeutic implications. JCI Insight. 2016;1(17):e89829.
13. Tong CC, Kao J, Sikora AG. Recognizing and reversing the immunosuppressive tumor microenvironment of head and neck cancer. Immunol Res. 2012;54(1–3):266–74.
14. Chen SMY, Krinsky AL, Woolaver RA, Wang X, Chen Z, Wang JH. Tumor immune microenvironment in head and neck cancers. Mol Carcinog. 2020;59(7):766–74.
15. Wondergem NE, Nauta IH, Muijlwijk T, Leemans CR, van de Ven R. The immune microenvironment in head and neck squamous cell carcinoma: On subsets and subsites. Curr Oncol Rep. 2020;22(8):81.
16. Aran D, Hu Z, Butte AJ. xCell: Digitally portraying the tissue cellular heterogeneity landscape. Genome Biol. 2017;18(1):220.
17. Eriksson M, Ambroise G, Ouchida AT, Lima Queiroz A, Smith D, Gimenez-Cassina A, Iwanicki MP, Muller PA, Norberg E, Vakifahmetoglu-Norberg H. Effect of mutant p53 proteinS on glycolysis and mitochondrial metabolism. *Mol Cell Biol* 2017, 37(24).
18. Principe N, Kidman J, Goh S, Tilsed CM, Fisher SA, Fear VS, Forbes CA, Zemek RM, Chopra A, Watson M, et al. Tumor infiltrating effector memory antigen-specific CD8 + T Cells Predict Response to Immune Checkpoint Therapy. Front Immunol. 2020;11:584423.
19. Liu Q, Sun Z, Chen L. Memory T cells: Strategies for optimizing tumor immunotherapy. Protein Cell. 2020;11(8):549–64.
20. Lechien JR, Descamps G, Seminerio I, Furgiuele S, Dequanter D, Mouawad F, Badoual C, Journe F, Saussez S. HPV involvement in the tumor microenvironment and immune treatment in head and neck squamous cell carcinomas. *Cancers (Basel)* 2020, 12(5).
21. Wang J, Sun H, Zeng Q, Guo XJ, Wang H, Liu HH, Dong ZY. HPV-positive status associated with inflamed immune microenvironment and improved response to anti-PD-1 therapy in head and neck squamous cell carcinoma. Sci Rep:. 2019;9(1):13404.

22. Krishna S, Ulrich P, Wilson E, Parikh F, Narang P, Yang S, Read AK, Kim-Schulze S, Park JG, Posner M, et al. Human papilloma virus specific immunogenicity and dysfunction of CD8 + T Cells in Head and Neck Cancer. Cancer Res. 2018;78(21):6159–70.
23. Fridman WH, Petitprez F, Meylan M, Chen TW, Sun CM, Roumenina LT, Sautès-Fridman C. B cells and cancer: To B or not to B? *J Exp Med* 2021, 218(1).
24. Wieland A, Patel MR, Cardenas MA, Eberhardt CS, Hudson WH, Obeng RC, Griffith CC, Wang X, Chen ZG, Kissick HT, et al: Defining HPV-specific B cell responses in patients with head and neck cancer. *Nature* 2020.
25. Kim SS, Shen S, Miyauchi S, Sanders PD, Franiak-Pietryga I, Mell L, Gutkind JS, Cohen EEW, Califano JA, Sharabi AB. B cells improve overall survival in HPV-associated squamous cell carcinomas and are activated by radiation and PD-1 blockade. Clin Cancer Res. 2020;26(13):3345–59.
26. Chen B, Li H, Liu C, Xiang X, Wang S, Wu A, Shen Y, Li G. Prognostic value of the common tumour-infiltrating lymphocyte subtypes for patients with non-small cell lung cancer: A meta-analysis. PLOS ONE. 2020;15(11):e0242173.
27. Maibach F, Sadozai H, Seyed Jafari SM, Hunger RE, Schenk M. Tumor-infiltrating lymphocytes and their prognostic value in cutaneous melanoma. Front Immunol. 2020;11:2105.
28. Gao G, Wang Z, Qu X, Zhang Z. Prognostic value of tumor-infiltrating lymphocytes in patients with triple-negative breast cancer: A systematic review and meta-analysis. BMC Cancer. 2020;20(1):179.
29. Kong JC, Guerra GR, Pham T, Mitchell C, Lynch AC, Warrier SK, Ramsay RG, Heriot AG. Prognostic impact of tumor-infiltrating lymphocytes in primary and metastatic colorectal cancer: A systematic review and meta-analysis. Dis Colon Rectum. 2019;62(4):498–508.
30. Geissler K, Fornara P, Lautenschläger C, Holzhausen HJ, Seliger B, Riemann D. Immune signature of tumor infiltrating immune cells in renal cancer. Oncoimmunology. 2015;4(1):e985082.
31. de Ruiter EJ, Ooft ML, Devriese LA, Willems SM. The prognostic role of tumor infiltrating T-lymphocytes in squamous cell carcinoma of the head and neck: A systematic review and meta-analysis. Oncoimmunology. 2017;6(11):e1356148.
32. Spector ME, Bellile E, Amlani L, Zarins K, Smith J, Brenner JC, Rozek L, Nguyen A, Thomas D, McHugh JB, et al. Prognostic value of tumor-infiltrating lymphocytes in head and neck squamous cell carcinoma. JAMA Otolaryngol Head Neck Surg. 2019;145(11):1012–9.
33. Tsujikawa T, Kumar S, Borkar RN, Azimi V, Thibault G, Chang YH, Balter A, Kawashima R, Choe G, Sauer D, et al. Quantitative multiplex immunohistochemistry reveals myeloid-inflamed tumor-immune complexity associated with poor prognosis. Cell Rep. 2017;19(1):203–17.
34. Johnson DE, Burtness B, Leemans CR, Lui VWY, Bauman JE, Grandis JR. Head and neck squamous cell carcinoma. Nat Rev Dis Primers. 2020;6(1):92.
35. Fakhry C, Westra WH, Li S, Cmelak A, Ridge JA, Pinto H, Forastiere A, Gillison ML. Improved survival of patients with human papillomavirus-positive head and neck squamous cell carcinoma in a prospective clinical trial. J Natl Cancer Inst. 2008;100(4):261–9.

36. Kansy BA, Concha-Benavente F, Srivastava RM, Jie HB, Shayan G, Lei Y, Moskovitz J, Moy J, Li J, Brandau S, et al. PD-1 status in CD8 + T Cells Associates with Survival and Anti-PD-1 Therapeutic Outcomes in Head and Neck Cancer. Cancer Res. 2017;77(22):6353–64.
37. Clarke J, Panwar B, Madrigal A, Singh D, Gujar R, Wood O, Chee SJ, Eschweiler S, King EV, Awad AS, et al. Single-cell transcriptomic analysis of tissue-resident memory T cells in human lung cancer. J Exp Med. 2019;216(9):2128–49.
38. Savas P, Virassamy B, Ye C, Salim A, Mintoff CP, Caramia F, Salgado R, Byrne DJ, Teo ZL, Dushyanthen S, et al. Single-cell profiling of breast cancer T cells reveals a tissue-resident memory subset associated with improved prognosis. Nat Med. 2018;24(7):986–93.
39. Waki K, Yamada T, Yoshiyama K, Terazaki Y, Sakamoto S, Matsueda S, Komatsu N, Sugawara S, Takamori S, Itoh K, et al. PD-1 expression on peripheral blood T-cell subsets correlates with prognosis in non-small cell lung cancer. Cancer Sci. 2014;105(10):1229–35.
40. Badoual C, Hans S, Merillon N, Van Ryswick C, Ravel P, Benhamouda N, Levionnois E, Nizard M, Si-Mohamed A, Besnier N, et al. PD-1-expressing tumor-infiltrating T cells are a favorable prognostic biomarker in HPV-associated head and neck cancer. Cancer Res. 2013;73(1):128–38.

## Table

Due to technical limitations, table 1 is only available as a download in the Supplemental Files section.

## Figures

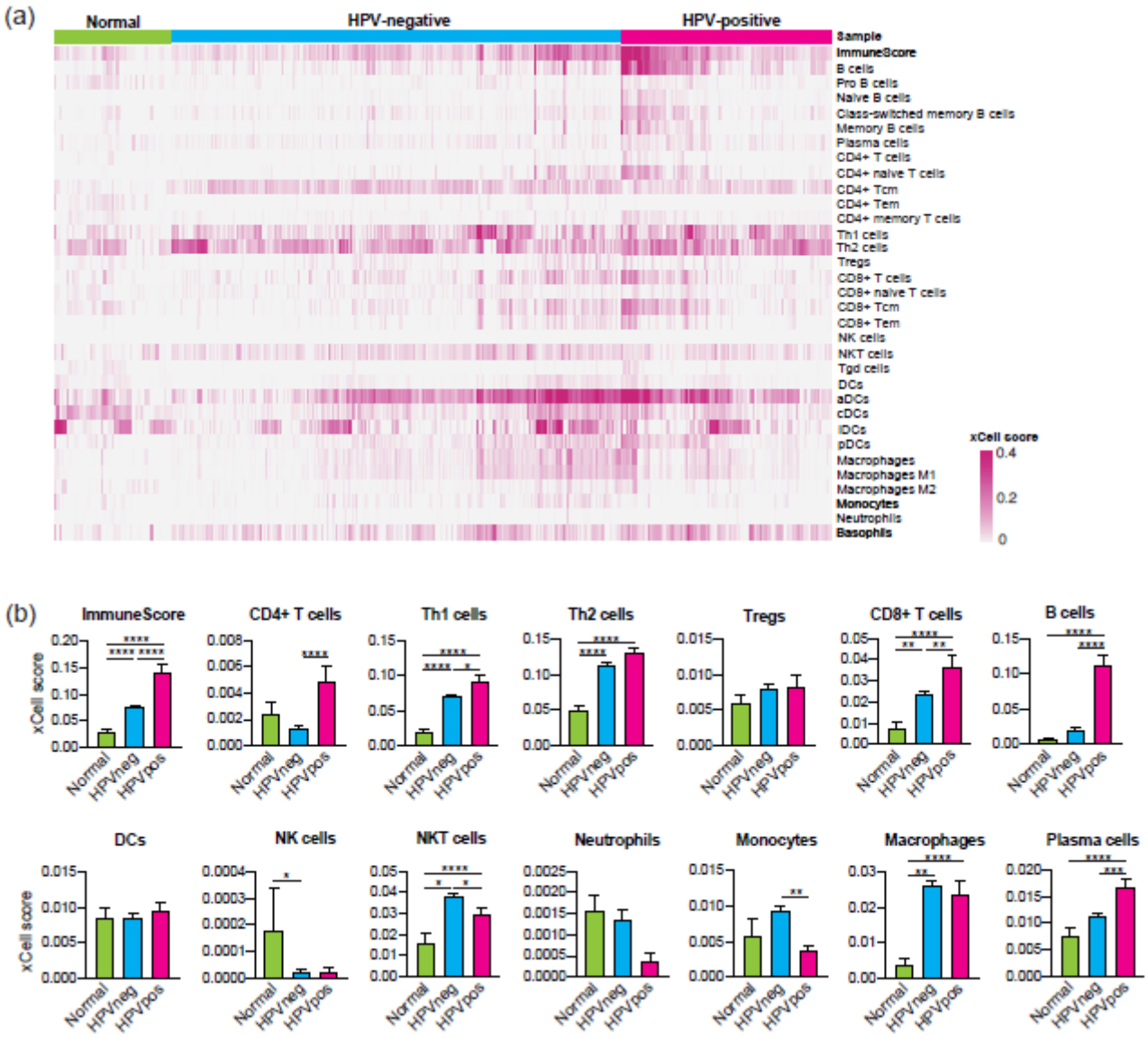


## Figure 1

Enrichment scores of 33 immune cell types in normal tissues and HNSCCs a, Heat map of xCell enrichment scores of 33 immune cell types in 44 normal tissues, 97 HPV-positive HNSCCs, and 423 HPV-negative HNSCCs. b, Bar graphs of enrichment scores of major immune cell types shown in a. HNSCC, head neck squamous cell carcinoma; HPV, human papillomavirus; HPVneg, HPV-negative; HPVpos, HPV-positive; DC, dendritic cells. *, P < 0.05; **, P < 0.01; ***, P < 0.001; ****, P < 0.0001.

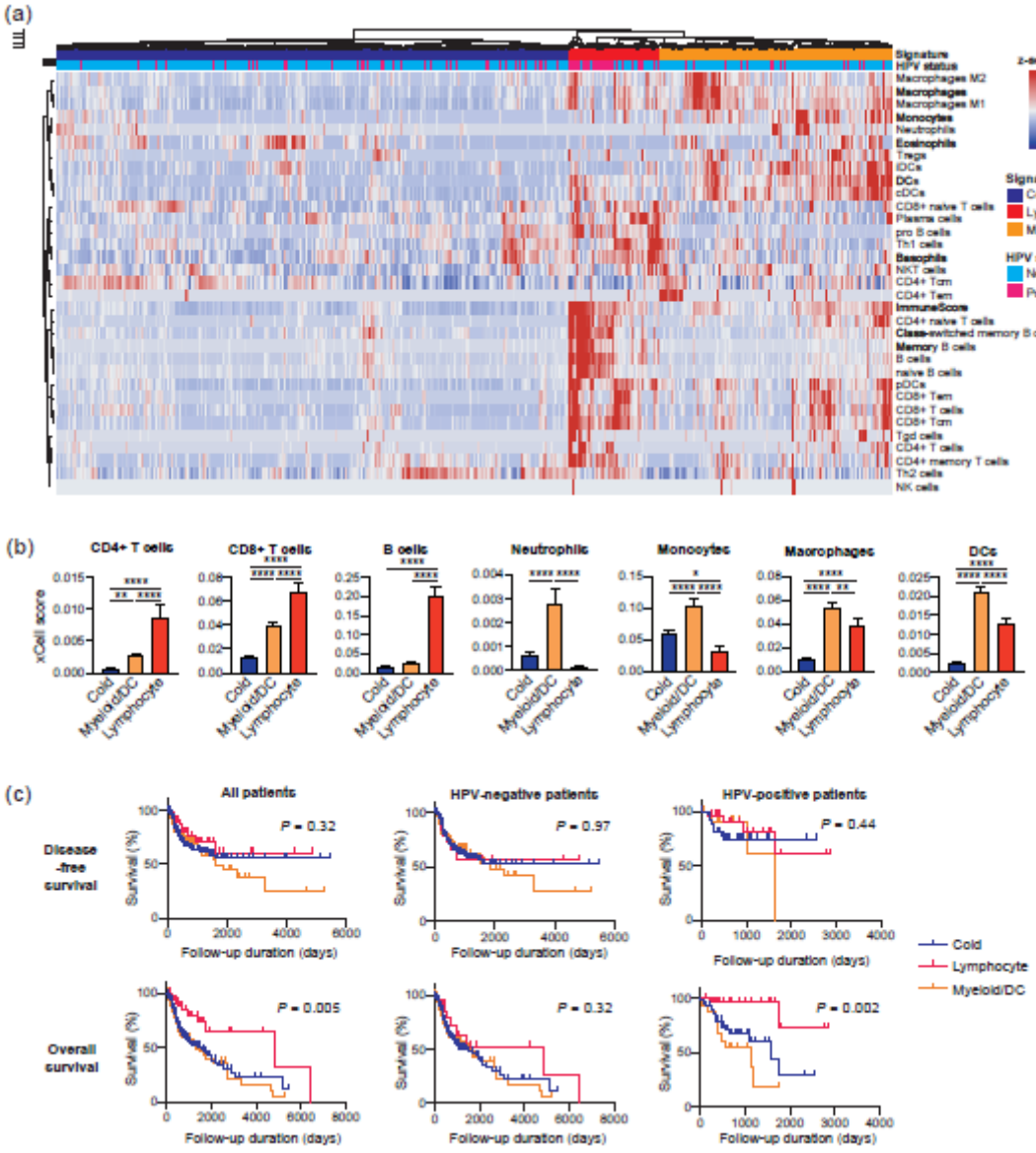


## Figure 2

The lymphocyte signature correlates with a favorable prognosis a, Heat map showing non-supervised hierarchical clustering of 520 HNSCCs based on enrichment scores of 33 immune cell types. b, Bar graphs of enrichment scores upregulated in the lymphocyte signature or myeloid/DC signature. c, Kaplan-Meier survival curves based on the three immune signatures. Disease-free survival was evaluated in all patients (n = 429), HPV-negative patients (n = 348), and HPV-positive patients (n = 81). Overall survival was evaluated in all patients (n = 495), HPV-negative patients (n = 403), and HPV-positive patients (n = 92). HNSCC, head neck squamous cell carcinoma; HPV, human papillomavirus; DC, dendritic cells. *, P < 0.05; **, P < 0.01; ****, P < 0.0001.

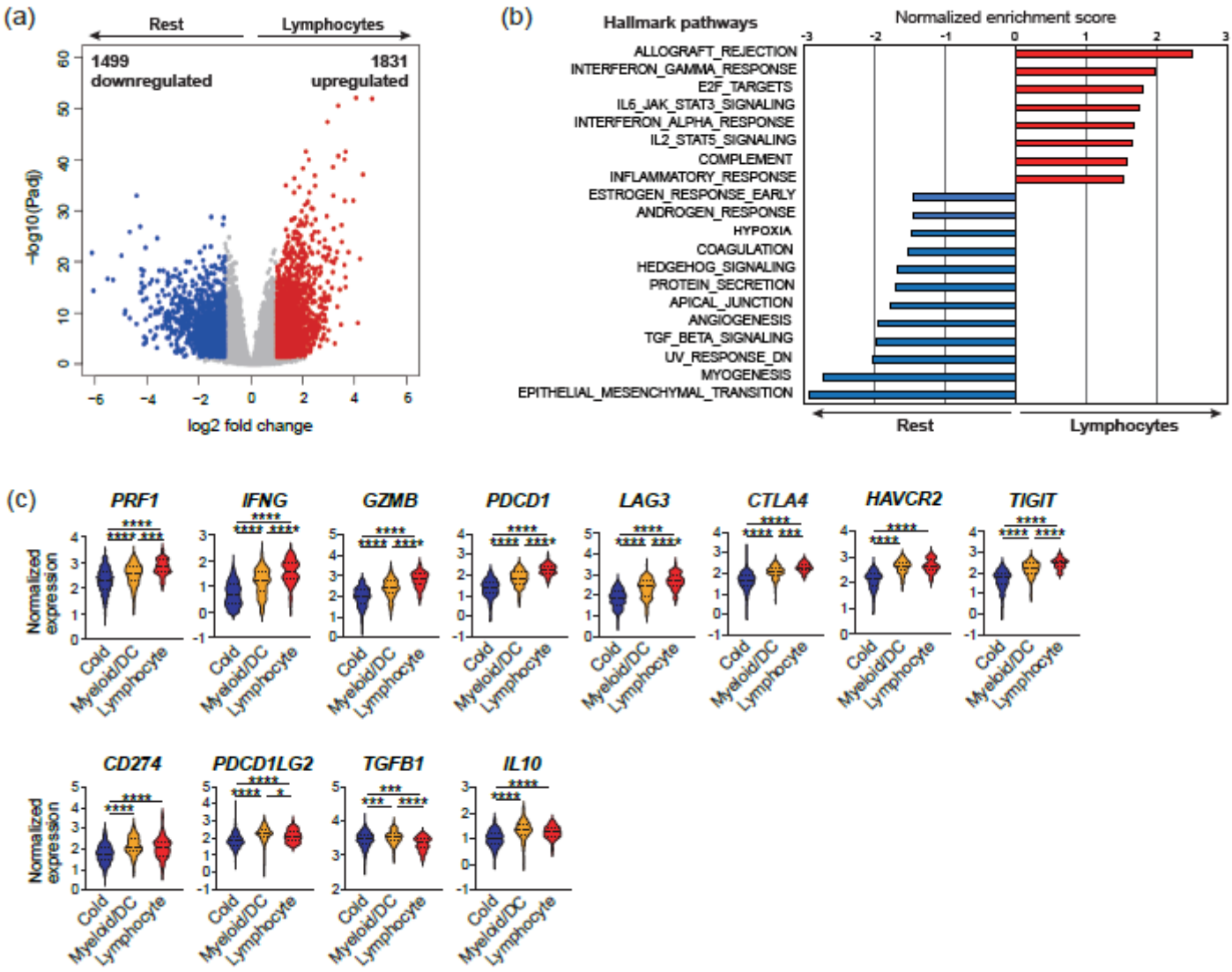


**Figure 3**

Differentially expressed genes and pathways across three immune signatures a, Volcano plot of differentially expressed genes in the lymphocyte signature. Red dots represent upregulated genes (Padj < 0.05, log2FC > 1), whereas blue dots represent downregulated genes (Padj < 0.05, log2FC < -1). b, Upregulated and downregulated hallmark pathways in the lymphocyte signature obtained by GSEA (FDR < 0.05). c, Violin plots of normalized expression of immune-related genes. GSEA, Gene set enrichment analysis; FDR, false discovery rate. *, P < 0.05; ***, P < 0.001; ****, P < 0.0001.

# Supplementary Files

This is a list of supplementary files associated with this preprint. Click to download.

- xCellSuppl.TableCCI.xlsx
- xCellSuppl.FiguresCCI.pdf

- xcellTableCCI.xlsx